Chapter 2: Synthesis and Characterization of Biodegradable and Functionally Superior Starch-Polyester Nanocomposites from Reactive Extrusion

2.1 Abstract

Biodegradable starch-polyester polymer composites are useful in many applications ranging from numerous packaging end-uses to tissue engineering. However the amount of starch that can form composites with polyesters without significant property deterioration is typically less than 25-30% because of thermodynamic immiscibility between the two polymers. A reactive extrusion process has been developed in this study in which high amounts of starch (approx. 40wt%) can be blended with a biodegradable polyester (polycaprolactone, PCL) resulting in tough nanocomposite blends with elongational properties approaching that of 100% PCL. We hypothesize that starch was oxidized and then co-polymerized/crosslinked with PCL in the presence of an oxidizing/crosslinking agent and modified montmorillonite (MMT) organoclay, thus compatibilizing the two polymers. Starch, PCL, plasticizer, MMT organoclay, oxidizing/crosslinking agent and catalysts were extruded in a co-rotating twin-screw extruder and injection molded. Elongational properties of reactively extruded starch-PCL nanocomposite blends approached that of 100% PCL at 3 and 6wt% organoclay. Strength remained the same as starch-PCL composites prepared from simple physical mixing without any crosslinking. X-ray diffraction results showed mainly intercalated flocculated behavior of clay at 1,3,6, and 9wt% organoclay. Scanning electron microscopy (SEM) showed that there was improved starch-PCL interfacial adhesion in reactively extruded blends with cross-linking than in starch-PCL composites without cross-linking. Dynamic mechanical analysis showed changes in primary α- transition temperatures for both the starch and PCL fractions, reflecting cross-linking changes in the nanocomposite blends at different

organoclay contents. The reactive extrusion concept can be extended to other starch-PCL like polymer blends with polymers like polyvinyl alcohol on one side and polybutylene succinate, polyhydroxy butyrate-valerate and polylactic acid on the other to create cheap, novel and compatible biodegradable polymer blends with increased toughness.

2.2 Introduction

Despite the fact that biodegradable polymer market has been active commercially for several years, it is in the initial stages of its product life cycle. The market for biodegradable polymers was approximately 20 million lbs in 2000 and expected to be 60 million lbs by 2005 (1). Much of the increase in consumption was expected to come from polyesters like polycaprolactone, polylactic acid etc. and their blends. A majority of market share for starch-based products is expected to be in loose fill packaging followed by compost bags, agricultural films, hygiene related products and paper coatings (1). Two main factors that can increase the market scope and size of biodegradable polymers are cost and material properties. Incorporating starch in polyester matrices can lead to improvements in stiffness, biodegradation kinetics and final material cost (2-4). These composites can also have net energy capacities comparable to fossil fuel-based plastics (1). However disadvantages associated with starch are as follows: i) immiscibility of native starch with all polyesters, ii) moisture absorption with time and iii) requires plasticizers particularly for flexible material applications. Rather than simple mixing of starch and polyesters, a reactive blend (RB) process is required to improve both interfacial phase adhesion between the two polymers and final material properties. In this paper, physical mixing will refer to

composites and RB/blends to compatible blends prepared from reactive extrusion. Our group has recently developed an extrusion process that addressed this challenge by reactively blending starch and polycaprolactone (PCL) (5).

Starch is one of the major components of cereal grains. Corn and wheat are major sources of commercial starches in the United States. Other sources include rice, potato, peas and tapioca. Starch is a mixture of two polysaccharides-amylose (linear 1,4-α-glucopyranosyl units) and amylopectin (linear 1,4-α-glucopyranosyl units and branched 1,6-α-glucopyranosyl units) (6). The amylose fraction has a degree of polymerization (DP) of $1x10^2$-$4x10^5$ and amylopectin has a DP of $1x10^4$-$4x10^7$ with the branches after every 19-25 linear units. Significant amounts of amylopectin (~ 75%) is present in most native corn and wheat starches, the rest being made up of amylose. However commercially available corn starches have amylose contents varying from 0% (waxy maize) to ~70% (high amylose) (6). So blends made from different starches will have different properties based on the ratio of branched to linear polymer fractions in the blend.

2.2.1 Biodegradable Starch-Polyester Composites and Blends

Biodegradable polyesters that can form mechanically compatible composites with starch are PCL, polybutylene succinate (PBS), polytetramethylene adipate-co-terephthalate (PAT), polyhydroxy butyrate-valerate (PHBV) and polylactic acid (PLA) (2, 4, 7-11). Many studies have been done on starch-PCL composites. Averoux *et al* (2), Mani *et al* (4) and Huang *et al* (11) reported that addition of starch to PCL caused an increase in modulus by a factor of 1.5-3, a decrease in strength by 50% and a very

large decrease in elongation to yield or break by a factor of 5-10. However at 25wt% amylose, PCL-amylose composites showed 5% less elongation at break, 10% less stress at break, and 20% less overall tensile strength than 100% PCL. Above 25wt% amylose for the 80000 molecular weight PCL, the strengths dropped off rather quickly, retaining less than one-half of their value at 50wt% amylose content. From dynamic mechanical and thermal analysis (DMTA), it was found that amylose was behaving as a phase separated, low particle size filler for the PCL. Studies done on starch-PHBV (12) composites also showed decrease in tensile strength upon incorporation of starch. Starch was also found to affect biodegradation kinetics by increasing the rate over that of polyesters alone (3-4). These studies (2, 4, 7-12) indicated that starch and polyesters were mechanically compatible but not thermodynamically and significant property deterioration took place at >25wt% starch. In fact starch-PCL composites and blends already exist in the market in various forms- MaterBi (composite) from Novamont SA (9-10), Envar (RB) from Michigan State University (13, 14) and Bioplast (composite) from Biotech Corp., Germany (15). Significant market potential exists for starch-based biodegradable blends that can be used in the applications mentioned before.

To increase the amount of starch that can be incorporated with polyesters without property deterioration, small amounts of compatibilizers are needed. Until now, these compatibilizers have been produced in two ways- a) Graft polymerization of polyester monomer on the starch backbone, or b) Addition of varying amounts of maleic anhydride (MA) modified polyester that is added to a starch-polyester matrix to produce a compatibilized blend. Graft polymerization techniques have been used in starch-PCL blends (7, 13, 14) only whereas maleic anhydride modifications have been

done on starch blends with PCL, PHBV, PBS and PAT (4, 16). For example one of the commercially available starch-PCL products (Envar) (13, 14) was synthesized through the first route. Narayan *et al* (14) reported tensile properties of RB blown films synthesized by polymerizing caprolactone monomer on starch. At final contents of 70wt% PCL and 30wt% plasticized starch, tensile strength showed an increase of 42%, but elongation decreased by atleast 59% over that of the control composite film. In another study Choi *et al* (7) reported that at starch:PCL ratios of 40:60, tensile strength, modulus decreased with increasing amounts of grafted compatibilizers. However elongation increased 8-fold over that of the composite at 30wt% compatibilizer, but was still 1/10 th of elongation of 100% PCL. They also found that grafted compatibilizers with short graft lengths and high degree of graft polymerization were the most effective. Many studies have been done on the second route too. Mani *et al* (4) reported a 3 and 1.5-fold increase in tensile strength of starch-PCL and starch-PBS blends respectively at 50wt% starch and 5wt% MA-modified polyester. However no changes in elongation or modulus were observed. No changes in tensile properties of starch-PAT blends were reported. Similarly Avella *et al* (16) reported a 3-fold increase in resilience of starch-PCL blends at 50wt% starch and 10wt% MA-modified polyester compatibilizer. But the resilience was still ½ of that of 100% PCL. They also reactively blended starch with PHBV through addition of organic peroxides. But no property changes were reported. Thus it is evident that graft polymerization and MA modification techniques do not work across the board for all polyesters (4, 7, 13, 16) and one property increase was offset by decrease in another property. Also these studies did not use plasticizers and their effects on reaction kinetics and overall properties were not evaluated.

2.2.2 A Novel Compatibilization Chemistry for Starch-Polyester Blends

Our research group has recently developed a unique reactive extrusion chemistry based on hydrogen peroxide (H_2O_2). H_2O_2 has been used for synthesis of fine chemicals including epoxidation of alkenes, hydroxylation of olefins, oxidative clevage of olefins, oxidation of alcohols, oxidation of carbonyl compounds etc (17). It has also been used in environmental applications including cyanide and nitrogen oxide control, control of reduced sulfur species, contaminated site remediation and waste-water treatment (17). We have not come across any polymer compatibilization chemistries based on hydrogen peroxide (inorganic peroxide) particularly on starch-based polymers. However there is a lot of compatibilization work on starch-based biodegradable plastics based on organic peroxides like benzoyl peroxide (BPO) or dicumyl peroxide (DCP) (18-25).

2.3 Materials

Starch

The primary starch used in our studies was native wheat starch (NWS) (MIDSOL 50, Midwest Grain Products, Atchison-Kansas). It had the following solids composition- 98.5% carbohydrates, 1% lipids, 0.2% proteins and 0.22-0.25% ash. Approximately 78% of carbohydrates in NWS was amylopectin (26). Other starch types were also used- native corn starch (NCS), high amylose corn starch (HACS) and waxy maize starch (WMS). NCS was C*Gel 03420 from Cerestar Inc., IN containing 78%

amylopectin (26); HACS was Cargill Amylogel 03003 from Cargill Inc., IA containing 70% amylose; WMS was C*Gel 04230 from Cerestar Inc, IN containing 99% amylopectin.

Polycaprolactone

CAPA 6806 (Solvay Caprolactones, Warrington-England) was a 80,000 molecular weight ($M_{n,average}$) polycaprolactone polymer available in the form of powder. TONE P787 was also a 80,000 molecular weight ($M_{n,average}$) polycaprolactone polymer obtained from Dow Chemical Company, CT and available in the form of pellets. These pellets were cryogenically ground into powder by a third party. Approximately 98% of powder sizes were less than 600 μm.

Montmorillonite Organoclay

Nanocor I.30E organoclay (Nanocor Inc., Arlington Heights, IL) is of montmorillonite (MMT) type with sodium ions (Na^+) replaced by quaternary ammonium octadecyl cations ($C_{18}H_{35}\ NH_4^+$). The structure of organoclay is given in Figure 2.1. MMT was available in powder form of average diameter of 13 μm. Each MMT platelet is made of two tetrahedral sheets with an octahedral sheet sandwiched in between. The tetrahedral sheets were made of silicon and oxygen while the octahedral sheets contained mainly oxygen, hydroxyls and larger cations like Al, Mg or Fe. Na^+ ions are present between two platelets in natural forms of MMT. However chemical processing could substitute these ions with required organic cations. The structure of MMT is illustrated in Figure 2.1. The distance between two sheets was denoted as d-spacing of first order (denoted by d_{001}).

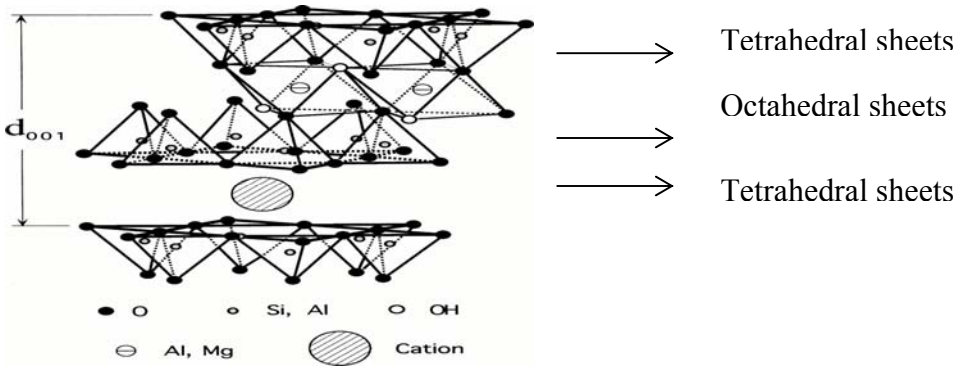

Figure 2.1: Structure of MMT organoclay (Nanomer I.30E) with inorganic cations replaced by organic ones.

Hydrogen Peroxide (H_2O_2)

Hydrogen peroxide was used as either 30% solution in water (Fluka Cheme GmbH, Switzerland) or 50% solution (FMC Corporation, TX) or >90% (FMC Corporation, TX). Additional catalyst compounds were also used and this included ferrous sulfate catalyst (Fischer Scientific, Fairlawn-NJ). Along with H_2O_2, the system became the well-known Fentons reagent. Hydrogen peroxide (30% solution) was used at a level of 0.067 ml/g starch unless otherwise mentioned. Ferrous catalyst was used at levels of 0.0025g/g to 0.07 g/g starch.

Glycerol (Mallinckrodt, Hazelwood-Missouri) was of atleast 99.9% purity and used as plasticizer. The formulations of starch-PCL blends at given levels of MMT organoclay are given in Table 2.1.

Table 2.1: Formulations used in synthesis of starch-PCL nanocomposites by reactive extrusion

Code	Starch %	PCL %	Glycerol %	Organoclay %	H_2O_2 ml/gram of starch*
STPCL	40	40	20	-	-
STPCLPER-0	40	40	20	-	0.067
STPCLPER-3	38.8	38.8	19.4	3	0.067
STPCLPER-6	37.6	37.6	18.8	6	0.067
STPCLPER-9	36.4	36.4	18.2	9	0.067

* H_2O_2 is 30% solution in water. If necessary **f**errous sulfate catalyst was used at 0.0025-0.07 g/g of starch on wet basis

2.4 Methods

2.4.1 Reactive Extrusion and Injection Molding

Ingredients (starch, PCL, glycerol, clay, peroxide and/or catalysts) were pre-mixed and fed to a conical co-rotating twin-screw microextruder (DACA Instruments, Goleta, California). The residence time was varied between 1-3 minutes and the melt was extruded out of the die in the form of cylindrical strands. The temperature throughout the extruder was kept at 120^0 C and screw speed at 110-116 rpm. The extruder barrel was blanketed with nitrogen during extrusion. Two batches of each formulation were extruded to ensure reproducibility. The extruded strands were injection molded in a micro-injector (DACA Instruments, Goleta, California) in the form of dog-bone pieces. The barrel was kept at 150^0 C and the mold was kept at ambient temperature.

2.4.2 Tensile Properties

Tensile measurements of dog-bone pieces were done on an Instron 1122 (Instron Corp., MA) universal tester at a crosshead speed of 50mm/min. Maximum stress, % elongation at rupture and Youngs Modulus (secant modulus) were measured. Secant modulus was calculated for stress-strain data at 1% strain.

2.4.3 Scanning Electron Microscopy (SEM)

SEM was used to analyze the domain structure of starch phase in starch-PCL composites and nanocomposite blends. Molded samples were ultra-sonicated for 5 minutes in warm water at 40^0 C. The samples were then analyzed with a Leica 440 scanning electron microscope (Leica Microinstruments Inc., IL) at electric field strength of 10 kV.

2.4.4 X-ray Diffraction

Clay dispersion behavior was studied by wide-angle x-ray diffraction (Scintag theta-theta wide angle x-ray diffractor working at 40 kV and 30 mA). Flat molded samples were used in diffraction analysis. The sample was scanned from 1 to 12^0 using a scan rate of 2^0/min unless otherwise mentioned.

2.4.5 Thermal Properties- Differential Scanning Calorimetry

Molded samples were analyzed by differential scanning calorimetry (DSC) (DSC 2920, TA Instruments, New Castle, DE) to determine PCL crystal properties. Approximately 3-10 mg of molded samples were placed in aluminium pans, which were then sealed. For crystallization experiments the sample was rapidly heated to

120^0 C and equilibrated for 3 minutes. Then it was cooled to 0^0 C at the rate of 10^0 C/min. For melting and crystallinity experiments, the samples were rapidly heated to 120^0 C, equilibrated for 3 minutes, then quenched to 0^0 C, held for 3 minutes and heated to 120^0 C at 10^0 C/min. The maximum of melting endothermic and exothermic crystallization peaks were taken as the melting point (T_m) and crystallization temperature (T_c) respectively and melting peak areas were used to calculate the enthalpy of fusion (ΔH_f) and percentage crystallinity. The peak areas were measured by sigmoidal baseline integration between 40^0C and 65^0C. The crystallinity, X_c of the PCL component in the composite and RB nanocomposites were obtained according to the following relation:

$X_c = \Delta H_f/(w \times \Delta H_{f,\ 100\%})$,

where $\Delta H_{f,\ 100\%}$ and ΔH_f indicate the heats of fusion for a 100% crystalline PCL and PCL in the samples respectively, w was the weight fraction of PCL in the sample. The heat of fusion of 100% crystalline PCL was taken as 142 J/g (27).

2.4.6 Dynamic Mechanical Analysis (DMA)

Dynamic viscoelastic properties of molded nanocomposites were measured with a Perkin-Elmer DMA 7e (Perkin Elmer Instruments, Shelton, CT). Molded samples of 1.5 x 4.0 x 10 mm^3 were analyzed in the 3-point bending mode. Storage modulus (E'), loss modulus ($E^{"}$) and phase angle shift δ were measured at a frequency of 1.6 Hz and a scan rate of 4^0/minute from -120^0 C to 52^0 C.

2.4.7 Carbonyl and Carboxyl Content in Oxidized Starch

2.4.7.1 Carboxyl Determination

A dry sample (~1 g) is slurried in water (100 ml) and 0.975 M NaOH is added to keep the pH above 10. After stirring for 1 hour, the mixture is back-titrated with 0.118 M HCl to the phenolphthalein end-point (pH 8.3). Composites with no peroxide are used as a control.

2.4.7.2 Carbonyl Determination

A dry sample (~1 g) is slurried in water (300 ml) and heated to boiling to completely solubilize it. The cooled solutions are adjusted to pH 3.2 with 0.118 M HCl and 60.0 ml of a hydroxylamine hydrochloride solution (HMH) is added (HMH, 25 g; 100 ml 0.5 M NaOH diluted to 500 ml). The solutions are heated to 40^0 C in an oven for 4 hours and titrated rapidly to pH 3.2 with 0.118 M HCl. A water sample is used as a control.

Calculation: % (C=0) = 0.118 x 0.028 x (ml control – ml sample) x 100

2.5 Results and Discussion

2.5.1 Tensile Properties

The tensile properties of starch-PCL (TONE P787) composites and nanocomposite blends were given in Table 2.2. Ferrous sulfate catalyst was used at a level of 0.0025g/g starch. Compared to 100% PCL, addition of starch at ratio of 1:1 with PCL decreased strength and elongation by more than 50% in the STPCL composites.

Compared to STPCL composites, elongation was dramatically improved in RB nanocomposites. Elongation approached that of 100% PCL at clay levels of 3 and 6% and 9% with lower elongation at 9% clay. The increase in elongation can be attributed to better interfacial adhesion between starch and PCL. Better interfacial adhesion was

Table 2.2: Tensile properties of starch-PCL blends and composites from reactive extrusion

Material	**Max. Strength, MPa**	**Ultimate Elongation, %**	**Tensile Modulus (secant) at 1% Strain, MPa**
100% PCL	30.8 (0.6)	1163 (22.0)	303.3 (42.3)
STPCL (non-reactive extrusion)	12.6 (1.2)	265.0 (95.3)	211.0 (13.8)
STPCLPER-0	3.2 (0.8)	200 (18.2)	36.5 (15.0)
STPCLPER-3	13.9 (0.7)	1197 (42.7)	263.4 (14.7)
STPCLPER-6	14.0 (0.7)	1074 (66.8)	253.4 (27.7)
STPCLPER-9	9.5 (1.1)	913 (58.1)	210.5 (31.5)

Number in brackets denote standard deviation

similarly associated with improved elongation in a RB study by Choi *et al* (7). Reactive blends containing no nanoclay (STPCLPER-0) showed poor properties with strength, elongation and modulus significantly lower than STPCL composites.

In the RB nanocomposites with 3 and 6% clay, the strength approached that of STPCL composites. Strength of STPCLPER-9 was significantly lower than those of STPCLPER-3/6 or STPCL. STPCLPER-3, and 6 showed higher modulus than STPCL and the same modulus as 100% PCL. Modulus of STPCLPER-9 was slightly lower than that of blends with 3wt% nanoclay. Increase in modulus upon incorporation of nanoclay (STPCLPER-3 & 6) was typical of filler systems because of high modulus of nanoclay materials (1 GPa) (28).

We hypothesize that during the extrusion RB process a small amount of cross-linked species were formed. This could include starch-starch, PCL-PCL and starch-PCL cross-links. However only starch-PCL cross-links were expected to improve starch-PCL interfacial adhesion while intra-molecular cross-links would decrease it (11). Tensile results indicated that starch-PCL cross-links might predominate rather than other types of cross-links. Also glycerol might play an important role in cross-linking. It is known yet if there exists a system in which starch, PCL and glycerol are cross-linked together and if so how much cross-linking is present. As will be discussed later, DSC and DMA results reflected cross-linking changes between nanocomposites at varying clay levels.

Varying the residence time between 1 and 3 minutes did not affect RB material properties. Also changing catalyst level between 0.0025 to 0.07 g/g starch did not

affect the tensile properties in these reactive blends. Table 2.3 illustrates the tensile properties of STPCLPER-6 at different ferrous catalyst levels.

Table 2.3: Tensile properties of STPCLPER-6 RB's at different ferrous sulfate catalyst levels.

Catalyst Level (g/g starch)	**Max. Strength, MPa**	**Ultimate Elongation, %**	**Tensile Modulus (secant) at 1% Strain, MPa**
0.0025	14.0 (0.7)	1074 (66.8)	253.4 (27.7)
2 x 0.0025	13.1 (0.6)	1142 (102.5)	206.6 (15.9)
3 x 0.0025	15.3 (0.8)	1175 (51.8)	235.2 (21.9)
28 x 0.0025	14.1 (0.8)	1011 (84.7)	236.8 (21.9)

Number in brackets denote standard deviation

In summary we have developed a reactive extrusion process to produce tough starch-PCL polymer blends than what exists in the market today (Novamont's Mater-Bi and Michigan State's Envar). This concept can be extended to different types of polymers

containing hydroxyl groups on one side and different types of polyesters (biodegradable and non-biodegradable) on the other side to tailor RB nanocomposites with application-specific properties.

2.5.2 Reaction Mechanism

H_2O_2 has a solution pH of 3.9 (30% solution), 2.8 (50% solution) and 0.9 (>90% solution) at 25^0C (17). When the solution pH > 2.4, H_2O_2 dissociates into perhydroxyl anions. The extent of dissociation depended on temperature and solution pH at that temperature. The dissociation is shown below:

H_2O_2 (aq) $\rightleftharpoons$ $H^+ + OOH^-$ (perhydroxyl anion) (pH >2.4) (17)

Reactive species from H_2O_2 can be formed in three ways depending on various conditions:

a) Undissociated H_2O_2: This form would be prevalent in the absence of any water or pH's less than 2.4. Undissociated peroxide behaved as a nucleophile and could readily add to electrophilic starch hydroxyls or PCL end-group hydroxyls giving rise to hydroperoxides. The peroxide nucleophile can also react with electrophilic PCL ester bonds in the backbone or PCL end carboxylic groups to give intermediate percarboxylic acids. Both hydroperoxides and percarboxylic acids have been found to readily initiate several reactions-epoxidation of alkenes, oxidation of alcohols, aldehydes and ketones, hydroxylation of olefins and others (17). These hydroperoxides could subsequently decompose at extrusion temperatures of 120^0C or higher to yield free radicals that could take part in further reactions. Formation of

hydroperoxides and percarboxylic acids are illustrated in Figure 2.2 a and b respectively. Thermal homolysis of hydroperoxides and percarboxylic acids are shown in Figure 2.2-c.

b) Dissociated H_2O_2: Above pH 2.4, H_2O_2 could dissociate to perhydroxyl anion (shown above) that was more nucleophilic than undissociated H_2O_2. This nucleophilic anion behaved the same way as undissociated H_2O_2 towards electrophilic groups like starch and PCL hydroxyls, PCL ester and end carboxylic groups.

c) Homolysis of O-O bond in H_2O_2: The O-O bond in H_2O_2 is relatively weak, approximately 213 kJ/mol (17), and is susceptible to homolysis by a variety of methods including thermal. Thus homolytic fission could be brought about by extrusion temperatures of 120^0 C. The reactive species produced by the homolytic fission is the hydroxy radical ($OH^{\cdot}$) that is second only to fluorine in terms of oxidizing power. The reaction is illustrated in Figure 2.2-d.

d) Ferrous Activated H_2O_2: H_2O_2 can decompose in the presence of ferrous ions (Fe^{2+}) to yield hydroxy radical ($OH^{\cdot}$) that could participate in further reactions. This reaction is illustrated in Figure 2.2-e.

The abundance of reactive functional groups present in the form of starch hydroxyls and PCL carbonyls/esters and PCL end-chain carboxyls and hydroxy groups raises the possibility of number of reactions. Some of the major compounds that have been

found to be formed in similar systems containing hydroxyl and carbonyl groups along with peroxides are:

i) Oxidized starch from oxidation of starch hydroxyls to carbonyls and carboxylic acids (Figure 2.3-a)

ii) Cross-linked oxidized starch-PCL through free radical chain mechanisms (Figure 2.3-b)

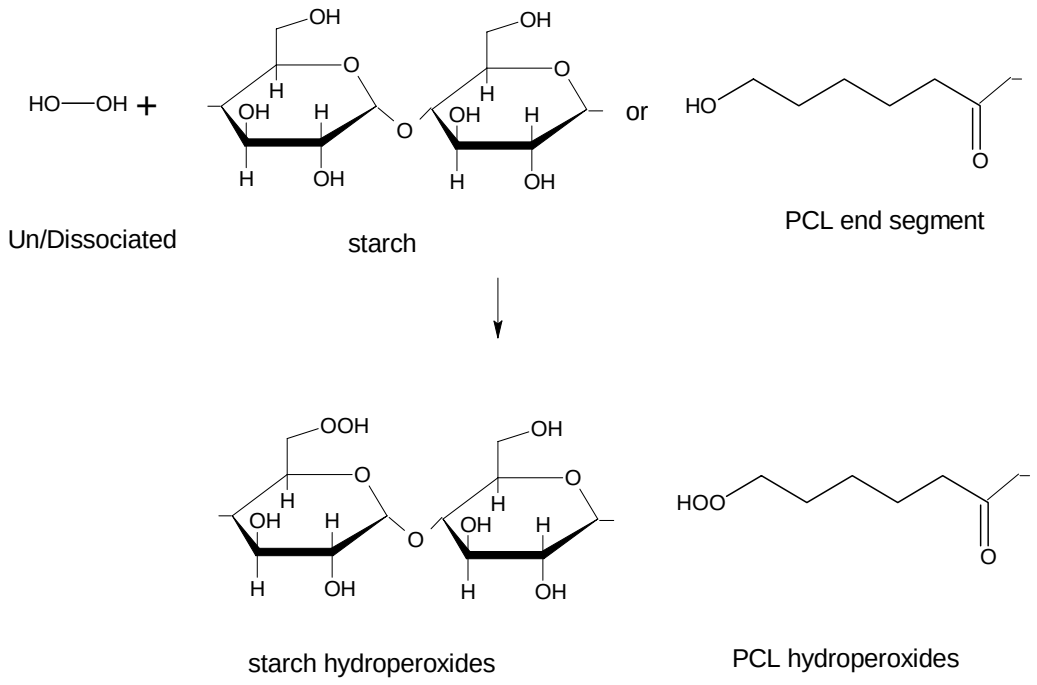

(a)

Figure 2.2: Formation of reactive species from H_2O_2 under different conditions by a) reaction of undissociated/dissociated peroxide with PCL electrophilic starch/PCL hydroxyls to yield hydroperoxides, b) reaction of undissociated/dissociated peroxide with electrophilic PCL esters or end-carboxylic groups to yield percarboxylic acids, c) homolysis of hydroperoxides and percarboxylic acids, d) thermal homolysis of H_2O_2 to hydroxy radicals and e) H_2O_2 activation by ferrous catalyst to yield hydroxy radicals.

Figure 2.2 (continued)

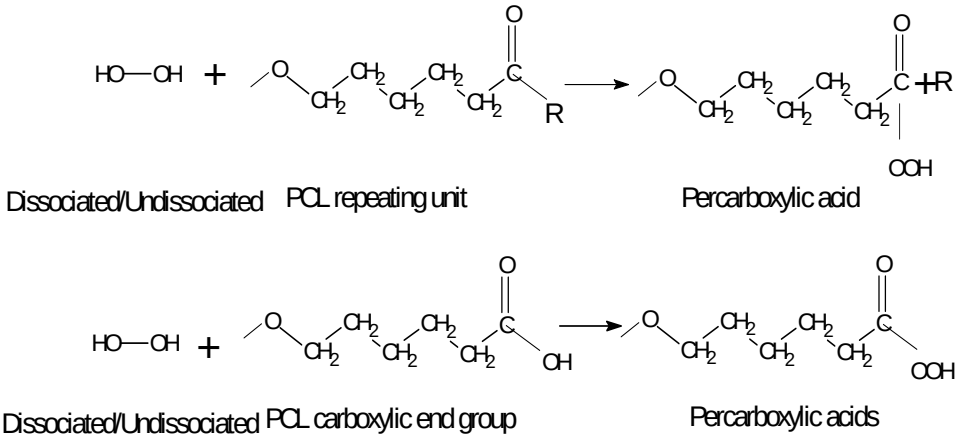

(b)

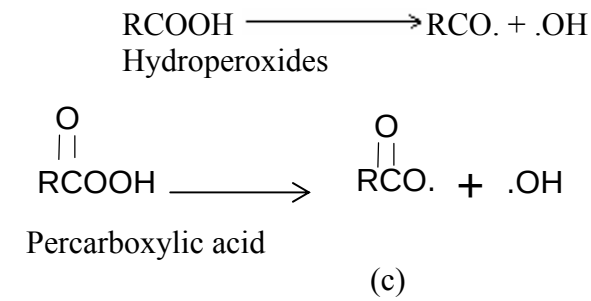

(c)

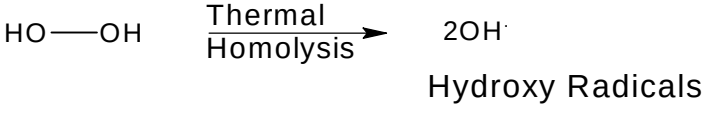

(d)

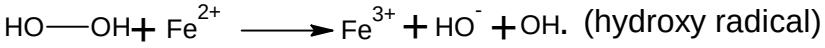

(e)

iii) Low molecular weight starch dextrins or low molecular weight PCL by chain scission

iv) Intra-polymer cross-linked compounds, i.e. starch-starch or PCL-PCL

Clearly products iii and iv are undesirable because of low mechanical property effects associated with degraded products.

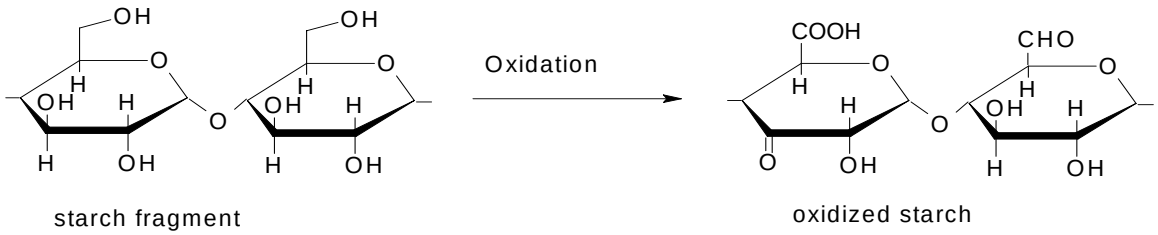

(a)

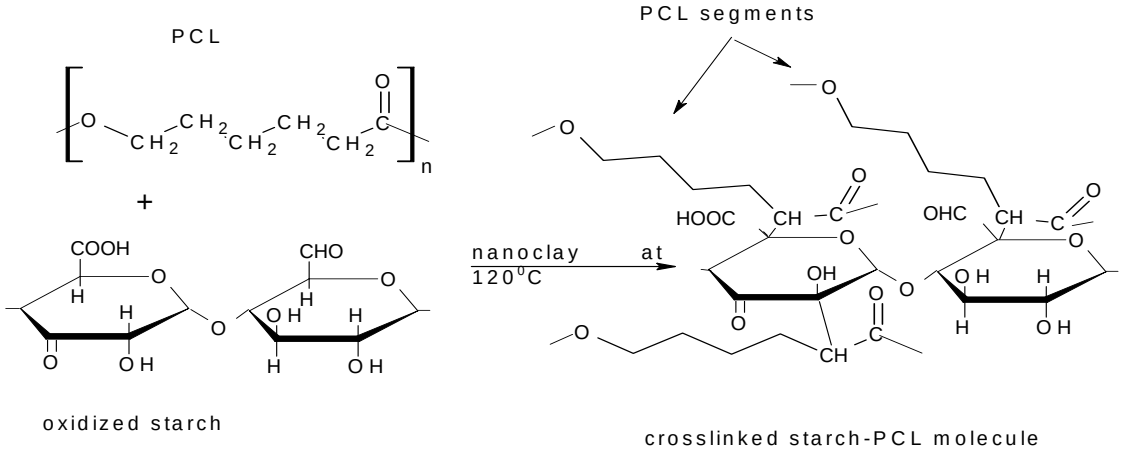

(b)

Figure 2.3: a) Oxidation of starch by hydrogen peroxide to yield aldehyde, keto or carboxylic groups, b) cross-linking between PCL and oxidized starch at the α-carbon atom to the carbonyl carbon.

2.5.3 Effect of Catalysts

Hydroxy radicals ($OH^{\cdot}$) generated by peroxide activation by ferrous sulfate were highly reactive and non-specific in their mode of action. Thus it was expected that these radicals played a small role during the reactive extrusion process. Table 2.4 shows a small reduction in strength of RB's with 6% nanoclay without any catalysts and no change in elongation and modulus. However hydroxy radicals generated by thermal homolysis or by homolysis of hydroperoxides/percarboxylic acids could still play a role during the reactive extrusion process of RB's in the absence of catalysts.

Table 2.4: Tensile properties of STPCLPER-6 with and without ferrous sulfate catalyst

STPCLPER-6	**Max. Strength, MPa**	**Ultimate Elongation, %**	**Tensile Modulus (secant) at 1% Strain, MPa**
With Catalyst	14.0 (0.7)	1074 (66.8)	253.4 (27.7)
Without Catalyst	11.1 (0.9)	1029.8 (28.7)	224.6 (12.9)

Number in brackets denote standard deviation

2.5.4 Morphology

SEM pictures of STPCL, STPCLPER-3 and STPCLPER-6 are shown in Figure 2.4. The pictures were obtained from molded samples that were ultra-sonicated in water for 5 minutes at 40^0 C. The pictures were magnified 2000 times. Even though starch is a hydrophilic polymer it is not possible to etch the polymer by immersing it in water. Ultrasonication aids in the etching process of hydrophilic starch from its domain in the starch-PCL polymer matrix into surrounding water. As seen in Figure 2.4, STPCL picture showed large void spaces in place of starch whereas STPCLPER-3 and STPCLPER-6 showed little voids. Starch in STPCL composites was immiscible with PCL as expected and showed easy separation from its domains. However in the RB nanocomposites with organoclay, there was better interfacial adhesion that resulted in no phase separation of starch upon ultrasonication. Choi *et al* (7) observed similar results for starch-PCL blends compatibilized with a starch grafted PCL copolymer. In the present study, the improved interfacial adhesion came from intermolecular starch-PCL cross-linked species that acted as a compatibilizer between uncross-linked starch and PCL.

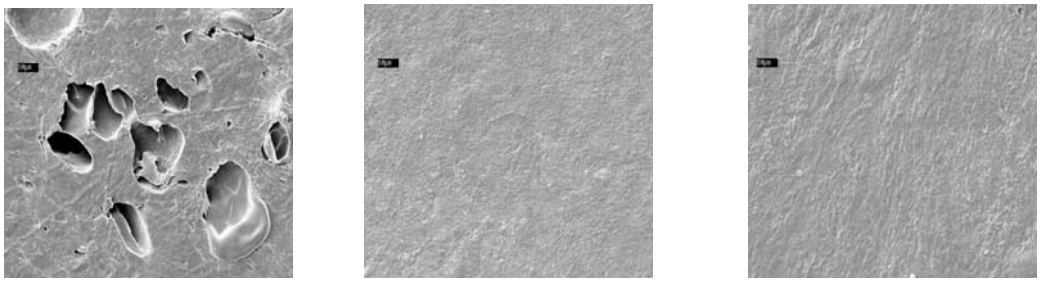

(a) (b) (c)

Figure 2.4: SEM pictures of ultrasonicated samples (from left to right): a) STPCL, b) STPCLPER-3 and c) STPCLPER-6 showing increasing interfacial adhesion between starch and PCL.

2.5.5 Dispersion of Organoclay

Figure 2.5-a shows the diffraction spectra of 100% Nanomer I.30 E clay. There was one peak, with d(001) spacing (see Figure 2.1) of 23 A. Figures 2.5 b-d show the spectra of 3,6 and 9wt% clay RB nanocomposites. There was one peak at 18.9-19.4 A that increased in intensity with increasing clay content. Also there was an additional peak seen in 9% clay spectra. The second peak in 9% clay had a d-spacing of 47.5 A although it was not completely resolved and appeared as a shoulder. The above data showed that organoclay was both intercalated and delaminated and less dispersion or decreased delamination was seen as clay level was increased to 9%. Compared to Nanomer 30E powder, peaks observed in RB's had lower d-spacing. This was contrary to the trend observed in typical polymer nanocomposites in which polymer chains were inserted between the clay sheets causing an increase in d-spacing. The presence of peak at 18.9-19.4 A in the RB nanocomposites with modified clay could be because some of the alkyl ammonium cations in the organoclay were leached out during the peroxide oxidation process.

2.5.6 Thermal Properties

PCL crystallization and melting point variations in starch-PCL composites and nanocomposite RB's are illustrated in Table 2.5. Crystallization temperature of RB nanocomposites increased between 1% to 9% organoclay, but remained lower than that of STPCL composites and 100% PCL. Crystallization temperature differences within the RB nanocomposites can be due to combination of two factors-

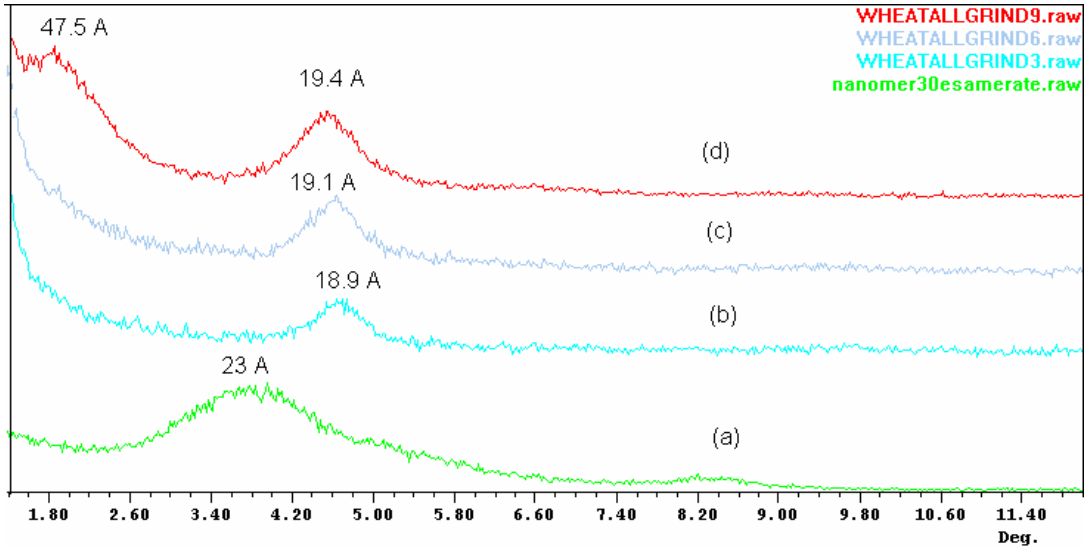

Figure 2.5: Wide angle X-ray diffraction spectra of a- Nanomer I.30E with d-spacing of 23 A and b, c, d, e- diffraction of RB's with 3%, 6% & 9% clay respectively.

i) Differences in cross-linking densities at different organoclay contents with higher cross-linking leading to lower crystallization temperature. Higher cross-linking will hinder structural relaxations of polymer molecules required for crystallization (11).

ii) Organoclay layers acting as nucleating agents causing a crystallization rate higher than that of STPCL (29). However the effective increase from nucleation can be offset by greater number of interactions between PCL and organoclay. These interactions will affect crystallization kinetics by hindering entropic changes that normally occur during crystallization (30). Thus overall the net increase in crystallization temperature of RB nanocomposite samples compared to STPCL was not very large as observed in other PCL-organoclay systems (29, 30).

Melting point of STPCL composites decreased slightly over that of 100% PCL. This can be attributed to a dilution and limited plasticizing effect arising from the presence of both starch and glycerol. However no large changes were found in RB samples over that of STPCL. This indicated that there were little changes in crystal type or size of the crystal in the presence of organoclay and reactive extrusion. Also no other endothermic peaks were observed upto 120^0 C. This suggested that most of the starch was destructurized and starch crystalline phase was lost.

Table 2.5: Melting and crystallization properties of starch-PCL composites and blends.

Material	Crystallization Temperature, T_c (^{0}C)	Melting Point, T_m (^{0}C)	% crystallinity	Relative crystallinity
100% PCL	27.40^{a}	57.59^{a}	30.10^{a}	1.00^{a}
STPCL	26.71^{b}	55.71^{b}	32.17^{a}	1.07^{a}
STPCLPER-1	20.77^{c}	54.18^{c}	27.10^{b}	0.90^{b}
STPCLPER-3	22.57^{d}	$55.50^{b,d}$	$28.85^{a,c}$	$0.96^{a,c}$
STPCLPER-6	23.60^{e}	$55.00^{b,d}$	$29.71^{a,c}$	$0.99^{a,c}$
STPCLPER-9	24.01^{e}	54.92^{d}	$30.37^{a,c}$	$1.01^{a,c}$

Number of replicates, n=6. Same letters indicate same mean and different letters indicate significant difference at α=0.05 by t-test for independent means

PCL crystallinity increased with increasing organoclay content and achieved the same level as that of STPCL at 3,6 and 9% organoclay contents. This indicated that cross-linking density differences in the nanocomposite systems at 3,6 and 9wt% organoclay

could not be statistically resolved on DSC. Thus significant improvements in tensile elongation were achieved from small amounts of starch-PCL cross-linking and the changes in mechanical properties were not due to changes in PCL crystalline morphology. Similar amounts of PCL crystallinity in STPCL and RB nanocomposites at 3,6, and 9wt% implied small amounts of cross-linking in them compared to uncross-linked PCL in STPCL composite. This has relevance to biodegradation rate too, as highly cross-linked PCL showed reduced biodegradation rates in other studies (3, 11).

2.5.7 Dynamic Mechanical Properties

Figure 2.6 shows tan δ peaks of 100% PCL, starch-PCL composites and RB nanocomposite blends. Salient features that were observed were as follows:

a) Presence of two α transitions in STPCL composites each corresponding to starch and PCL.

b) Increase in $(\tan \delta)_{max}$ of PCL peak in STPCL over that of 100% PCL.

c) Decrease in $(\tan \delta)_{max}$ of PCL and increase in $(\tan \delta)_{max}$ of starch peaks in STPCLPER-3&6 compared to those in STPCL.

d) Decrease in $(\tan \delta)_{max}$ of PCL and decrease in $(\tan \delta)_{max}$ of starch peaks with increasing organoclay content.

e) Changes in α transition temperatures of PCL and starch fractions within the RB nanocomposites.

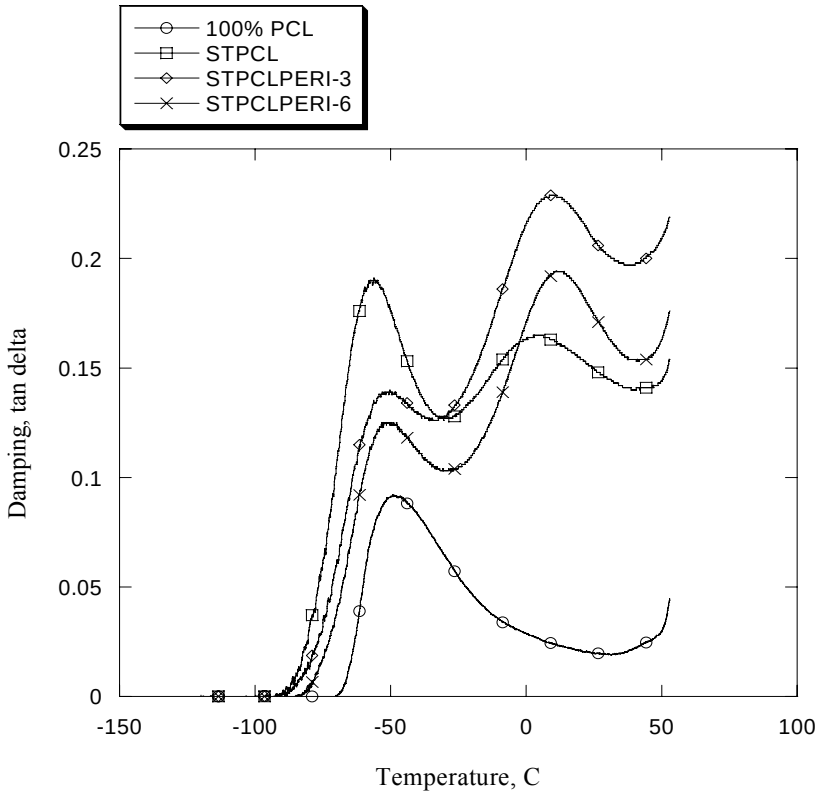

Figure 2.6: tan δ peaks of 100% PCL and starch-PCL blends. Each curve is average of 5-6 replicates.

Table 2.6 shows changes in α transition and peak damping values of 100% PCL, starch-PCL composites and RB nanocomposites. In STPCL, the transition of starch was broader compared to that of PCL since the amylopectin fraction of native starch is highly branched. This leads to a wide distribution in transition temperatures of starch corresponding to each population of starch molecule with different branching lengths and densities. In the presence of starch in STPCL samples, PCL α transition decreased. This can be attributed to a limited plasticizing effect of both glycerol and starch in the blend. This plasticizing effect also contributed to a small change in PCL melting point as was observed from DSC results in Table 2.5. The $(\tan \delta)_{max}$ of PCL

peak in STPCL increased over that in 100% PCL. A small part of this increase can be attributed to increasing mobility of PCL molecules because of plasticizing effect of starch and glycerol even though PCL crystallinity remained same both in 100% PCL and STPCL samples. Also other studies have shown secondary β transitions for starch-glycerol mixtures in the α transition region of PCL (2, 31). This could have led to a superimposition effect thus greatly increasing peak damping values in the PCL transition region.

RB samples showed increases in α transition temperatures for both the polymeric components- starch and PCL. As illustrated in Table 2.6, α transitions for RB's showed increases over that of STPCL. The transitions showed a decreasing trend with increasing organoclay level. However even at 9wt% organoclay the transitions were still higher than those in STPCL. The changes in α transition temperatures can be attributed to the following reasons:

Table 2.6: Damping behavior of starch-PCL blends. $T_{\alpha 1}$ and $T_{\alpha 2}$ are α transition temperatures of PCL and starch respectively and are measured at peak maximum.

Material	**$T_{\alpha 1}$, ^{0}C**	**$(\tan \delta 1)_{max}$**	**$T_{\alpha 2}$, ^{0}C**	**$(\tan \delta 2)_{max}$**	**Half Peak Width of Starch Relaxation, ^{o}C**
100% PCL	-51	0.092	-	-	-
STPCL	-57	0.191	4	0.164	29.9
STPCLPER-1	-49	0.144	15	0.234	22.6
STPCLPER-3	-51	0.139	10	0.223	22.5
STPCLPER-6	-51	0.124	11	0.194	23.9
STPCLPER-9	-54	0.124	10	0.185	24.7

Number of replicates, n= 5-6,

a) Comparing STPCL and RB's, the increase in polymer transition temperatures can be associated with cross-linking and/or co-polymerization effects (32). The increase in transition temperature indicated that cross-linking predominated rather than starch depolymerization that would decrease the transition temperature. Thus even though starch depolymerization was observed in a similar starch oxidation study by Wing *et al* (33), this did not decrease the starch transition temperature.

b) Within the RB nanocomposites, the transition temperature of starch and PCL decreased with increasing organoclay. One reason could be that the density of cross-linking decreased with increasing organoclay content. Organoclay, because of their high aspect ratio and surface area was expected to act as a significant physical barrier to cross-linking. Also, the decrease in α transition with increasing clay level cannot be associated with depolymerization effects, since starch oxidation levels showed decreasing trend with increasing organoclay level. The second reason could be that increased intercalation of PCL and starch with increasing organoclay content can decrease transition temperature. Similar decreases in glass transition of cross-linked epoxy nanocomposite systems were also reported in other studies (34, 35). The decrease would indicate that the polymer chains were not tied down on the surface of silicates. However since the present polymer system is affected by starch oxidation, cross-linking and polymer-organoclay interactions, the changes observed could be due to a combination of these three factors.

Comparing with STPCL, RB's showed interesting damping behavior. Decrease in $(\tan \delta)_{max}$ of PCL peak can be attributed to increased cross-linking and lesser fraction of

amorphous PCL. Oxidation of starch led to high $(\tan \delta)_{max}$ for the starch peaks in RB's.

Table 2.7 illustrates starch oxidation levels at different organoclay levels. Addition of organoclay at 3wt% decreased the amount of carboxyls while carbonyl content was the same. At 6 and 9wt% organoclay, both carboxyl and carbonyl content decreased further indicating lower oxidation. Under the reaction conditions, more carbonyls than carboxyls were formed than reported in a similar starch oxidation study (33). This could be because of easy accessibility of hydroxyl groups in H_2O_2 due to ease of starch gelatinization in the presence of glycerol and at elevated temperature. The $(\tan \delta)_{max}$ of PCL peak in the RB nanocomposites also decreased with increasing organoclay content. This change in PCL damping peak value may be caused by crystallinity differences even though these could not be statistically resolved on DSC

Table 2.7: Oxidation levels of starch in Starch-PCL RB's.

Material	-COOH, mmol/g,	-C=O, %
STPCLPER-3	0.55^{b}	6.7^{a}
STPCLPER-6	0.15^{c}	4.3^{b}
STPCLPER-9	0.16^{c}	5.1^{b}

Number of replicates, n= 3-4. Same letters indicate same mean and different letters indicate significant difference at α=0.05 by t-test for independent means

for nanocomposites at 3,6 and 9wt% organoclay. The decreases in $(\tan \delta)_{max}$ for both starch and PCL with increasing clay content can also be attributed to strong polymer-clay interactions. Weaker interactions and agglomeration of organoclay sheets have been known to increase damping because of higher friction between polymer and organoclay particles whereas strong interactions decreased damping (36, 37). Thus

overall damping of starch fraction is affected more by oxidation and polymer-clay interactions rather than cross-linking that will tend to decrease damping, while that of PCL fraction seems to be affected by cross-linking and polymer-clay interactions.

Starch α relaxation peak half-width in STPCL composite and RB nanocomposities are shown in Table 2.6. The widths in RB nanocomposites showed significant decrease over that in STPCL. This could not be caused by organoclay since unfilled systems like in STPCL are generally less broad than filled systems (38). The decrease in the peak widths of RB nanocomposites can explain their improved elongational properties to some extent. The broadening of α transition might be related to restrained chain mobility making molecular relaxations more difficult (39). This implied a greater intermolecular slippage in the nanocomposite RB's during tensile measurements before final rupture than in STPCL. Half-widths of PCL peaks could not be measured because the damping increased with increasing temperature before forming the whole peak.

Figure 2.7 shows the storage modulus (G') curves for STPCL composite and RB nanocomposites at 3,6 and 9 wt% organoclay. Storage modulus increased with increasing organoclay content in all regions. However the increases were small compared to those seen in uncross-linked PCL-organoclay systems (30, 40). The increase in G' with increasing organoclay was offset by decreasing cross-linking density as seen from α transition changes. Thus the overall increase was smaller than expected. Also in the glass-rubbery transition region G' of RB nanocomposites was higher than that of STPCL.

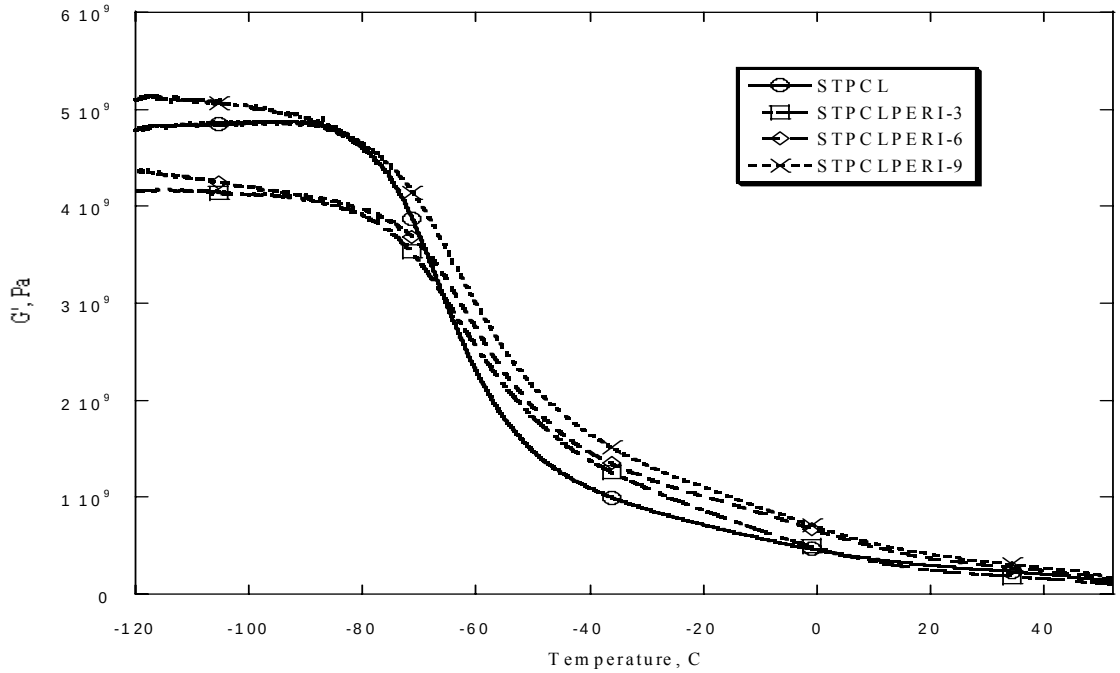

Figure 2.7: Storage modulus (G') of STPCL and RB nanocomposites at 3,6 and 9wt% organoclay. Each curve is a replicate of 5-6 replicates.

2.5.8 Effect of Starch Type

As mentioned before, starch could be produced from different crop varieties-corn, wheat, high amylose and waxy maize or high amylopectin. However corn and wheat starches were more widely available and cheaper ($0.18-0.33 /lb) than the other two ($0.40-0.50/lb). It was necessary to determine if PCL-like elongational properties observed in wheat starch-based RB's could be seen in other blends. Table 2.8 illustrates the tensile properties of starch-PCL (CAPA 6806) RB's containing 6wt% nanoclay. Overall best properties were observed for wheat starch. Table 2.9 shows the PCL crystallinity, melting point and onset melting temperatures for the RB's. From Table 2.9 it is clear that better tensile properties observed for blends with wheat or

corn starch could not be explained on the basis of any changes in PCL crystalline morphology.

Table 2.8: Tensile properties of STPCLPER-6 RB's based on different starch sources

STPCLPER-6	**Max. Strength, MPa**	**Ultimate Elongation, %**	**Tensile Modulus (secant) at 1% Strain, MPa**
Wheat Starch (NWS)	12.5 (0.9)	1169.1 (43.1)	219.7 (31.5)
Corn Starch (NCS)	11.7 (0.6)	1137 (67.4)	164.9 (6.1)
High Amylose Corn Starch (HACS)	8.7 (0.3)	53.9 (5.7)	173.2 (10.8)
Waxy Maize Starch (WMS)	6.4 (0.3)	507.4 (61.2)	160.4 (3.3)
Mix of HACS and WMS (approx. 75% amylopectin & 25% amylose)	6.2 (0.4)	371.5 (127.3)	170.8 (9.0)

Table 2.9: PCL melting properties in starch-PCL RB's containing 6% nanoclay from different starch sources.

Material	Melting Onset Temperature	Melting Point, T_m (^{0}C)	% crystallinity	Relative crystallinity
100% PCL	50.3[a]	55.6[a]	33.8[a]	1.00[a]
NWS	50.3[a]	56.7[a]	34.9[a]	1.03[a]
NCS	50.7[a]	56.6[a]	33.2[a]	0.98[a]
HACS	50.5[a]	56.5[a]	34.1[a]	1.01[a]
WMS	50.6[a]	56.5[a]	37.2[a]	1.10[a]
HACS+WMS with 75% amylopectin	50.1[a]	56.4[a]	34.0[a]	1.01[a]

NWS-native wheat starch, NCS-native corn starch, HACS- high amylose corn starch, WMS- waxy maize starch. Numbers with same alphabet denote no significant difference at α=0.05

PCL crystallinity properties were also studied by wide angle X-ray diffraction from 1-40^0 using a scan rate of 5^0/min. Figure 2.8 shows that the only peaks observed in the RB's were contributed by nanoclay ordering and PCL crystallinity. Two PCL crystallinity peaks were observed at 4.2 A and 3.8 A and these were unchanged in the RB's. This confirmed results from DSC essentially showing no changes in PCL crystalline morphology upon reactive extrusion. Also it can be seen from Figure 2.8 that there was no starch crystallinity in the RB's. Absence of other peaks in the RB's indicated that there was no residual granular structure and starch was present mainly in amorphous form in the RB's.

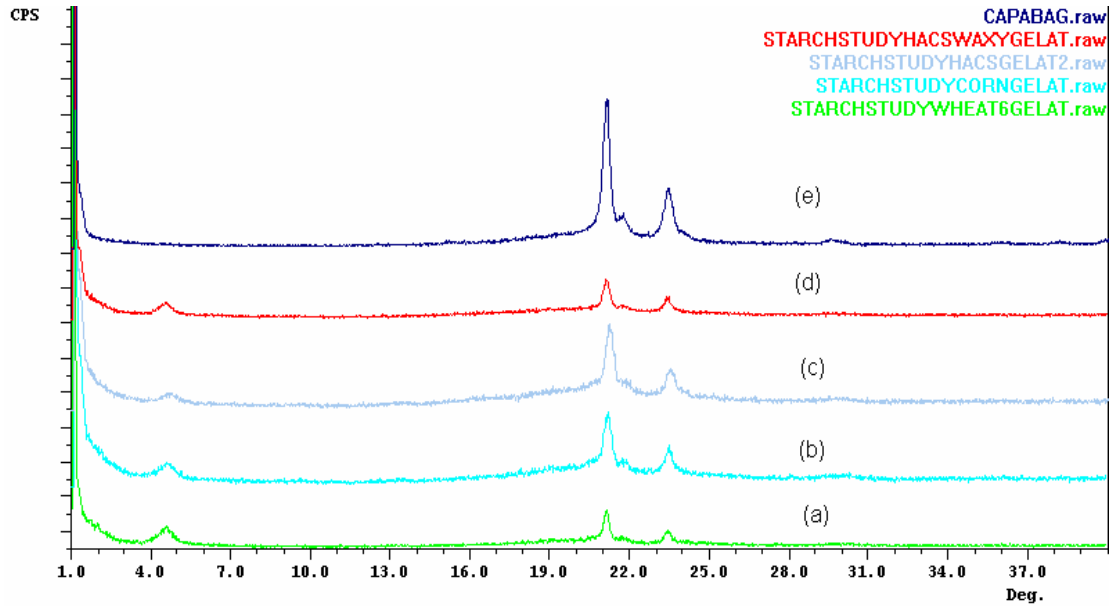

Figure 2.8: Wide angle X-ray diffraction of RB's containing 6% clay from different starch sources, a- wheat starch, b- corn starch, c- high amylose corn starch, d- mixture of high amylose and waxy maize. Figure 2.8-e shows diffraction spectra of 100% PCL.

2.6 Conclusion

A new reactive extrusion chemistry was developed to improve interfacial adhesion between starch and PCL. Fenton's reagent was used to oxidize starch as well initiate cross-linking between oxidized starch and PCL. The cross-linking step was catalyzed by a MMT organoclay having high surface area and aspect ratio. Elongation of these nanocomposites was comparable to that of 100% polyester. Strength and modulus remained the same as in starch-PCL composites without cross-linking. This reactive extrusion process can be extended to other starch-PCL like polymer blends with polymers like polyvinyl alcohol on one side and polybutylene succinate, polyhydroxy

butyrate-valerate and polylactic acid on the other to create cheap, novel and compatible biodegradable polymer blends with increased toughness.

2.7 References

1. Sclecterm, M., Biodegradable Polymers, Business Communications Company Inc., CT, USA (2001).

2. Averous, L., Moro, L., Dole, P., Fringant, C., Polymer, vol. 41, 4157(2000).

3. Tokiwa, Y., Iwamoto, A., Koyama, M., Polymer Preprints, vol. 63, 742 (1990).

4. Mani, R., Bhattacharya, M., European Polymer Journal, vol. 37, 515 (2001).

5. Kalambur, S., Rizvi, S.S.H., Polymer International, vol. 53, 1413 (2004).

6. Kaplan, D.L., Mayer, J.M., Ball, D., McCassie, J., Allen, A.L., Stenhouse, P. Fundamentals of Biodegradable Polymers, In Biodegradable Polymers and Packaging eds Ching, C., Kaplan, D., Thomas, E., Technomic Publishing Co., Pennsylvania, USA, pg. 1 (1993).

7. Choi, E.J., Kim, C.H., Park, J.K., Journal of Polymer Science Part B: Polymer Physics, vol. 37, 2430 (1999).

8. Willett, J.L., Shogren, R.L., Polymer, vol. 43, 5935 (2002).

9. Bastioli, C., Bellotti, V., Del Tredici, G., Guanella, I., Lombi, R., Complexed Starch-Containing Compositions having High Mechanical Properties, US Patent# 6348524 (1999).

10. Bastioli, C., Raffa, G., Rallis, A., Cotton Budsticks of Plastic Material, US Patent# 5902262 (1995).

11. Huang, S.J., Koenig, M.F., Huang, M., Design, synthesis and properties of biodegradable composites, In Biodegradable Polymers and Packaging, eds., Ching, C., Kaplan, D., Thomas, E., Technomic Publishing Company PA, USA, pg. 97 (1993).

12. Ramsay, B.A., Langlade, V., Carreau, P.J., Ramsay, J.A., Applied Environmental Microbiology, vol. 59, 294 (1992).

13. Dubois, P., Krishnan, M., Narayan, R., Polymer, vol. 40, 3091 (1999).

14. Narayan, R., Krishnan, M., Snook, J.B., Gupta, A., DuBois, P., US Patent# 5,969,089 (1999).

15. Bastioli, C. Polymer Degradation and Stability, vol. 59, 263 (1998).

16. Avella, M., Errico, M.E., Rimedio, R., Sadocco, P., Journal of Applied Polymer Science, vol. 83, 1432 (2002).

17. Jones, C.W., Applications of Hydrogen Peroxide and Derivatives, Royal Society of Chemistry, UK (1999).

18. Vaidya, U.R., Bhattacharya, M., Journal of Applied Polymer Science, vol. 52, 617 (1994).

19. Bhattacharya, M., Vaidya, U.R., Zhang, D., Narayan, R., Journal of Applied Polymer Science, vol. 57,539 (1995).

20. Mani, R., Bhattacharya, M., European Polymer Journal, vol. 34,1467 (1998).

21. John, J., Tang, J., Yang, Z., Bhattacharya, M., Journal of Polymer Science Part A-Polymer Chemistry, vol. 35,1139 (1997).

22. Bhattacharya, M., Mani, R., Tang, J., Journal of Polymer Science Part A-Polymer Chemistry, vol. 37,1693 (1999).

23. Carlson, D., Nie, L., Narayan, R., Dubois, P., Journal of Applied Polymer Science, vol. 72,477 (1999).

24. Mani, R., Bhattacharya, M., European Polymer Journal, vol. 37,515 (2001).

25. Dubois, P., Narayan, R., Macromolecular Symposium, vol. 198,233 (2003).

26. Bemiller, J.N., Whistler, R.L., Carbohydrates in Food Chemistry, ed. Fennema, O, R., Marcel Dekker Inc, USA (1996).

27. Wunderlich, B. Crystal melting, Macromolecular Physics, vol. 3, 54 (1980).

28. Nielsen, L.E., Lanel, R.F. Mechanical Properties of Polymers and Composites (chapter 8), Marcel Dekker Inc. NY USA, pg. 461 (1994).

29. Liu, X., Wu, Q. Polymer, vol. 42, 10013 (2001).

30. Di, Y., Iannace, S., Di Maio, E.D., Nicolais, L. Journal of Polymer Science Part B: Polymer Physics, vol. 41, 670 (2003).

31. Averous, L., Fauconnier, N., Moro, L., Fringant, C. Journal of Applied Polymer Science, vol. 76, 1117 (2000).

32. Nielsen, L.E., Lanel, R.F. Mechanical Properties of Polymers and Composites (chapter 4), Marcel Dekker Inc. NY USA, pg. 131 (1994).

33. Wing, R.E., Willett, J.L. Industrial Crops and Products, vol. 7, 45 (1997).

34. Massam, J., Pinnavaia, T.J. Material Research Society Symposium Proceedings, vol. 520 (1998).

35. Bajaj, P., Jha, N.K., Ananda Kumar, R.J. Journal of Applied Polymer Science, vol. 40, 203 (1990).

36. Gray, R.W., McCrum, N.G. Journal of Polymer Science, vol. **7,** 1329 (1969).

37. Nielsen, L.E. Transactions in Society of Rheology, vol. 13, 141 (1969).

38. Becker, O., Varley, R., Simon, G. Polymer, vol. 43, 4365 (2002).

39. Lin, M.S., Lee, S.T. Polymer, vol. 38, 53 (1997).

40. Jimenez, G., Ogata. N, Kawai. H., Ogihara, T. Journal of Applied Polymer Science, vol. 64, 2211 (1997).